Measurement of anisotropic flow for BES-II energies at RHIC from STAR

Sharang Rav Sharma[1,*] for the STAR Collaboration

[1]Department of Physics, Indian Institute of Science Education and Research (IISER) Tirupati, India

Abstract. Anisotropic flow reflects how the medium produced in heavy-ion collisions expands and responds to the initial geometry of the collision. The anisotropic flow coefficients, such as v_1 (directed flow), v_2 (elliptic flow), and v_3 (triangular flow), describe different aspects of this collective motion and are sensitive to the equation of state (EoS) of the created matter. In these proceedings, we report measurements of the flow coefficients using high-statistics data from the RHIC Beam Energy Scan (BES-II), collected with the upgraded STAR detector acceptance, for a broad range of hadron species. The experimental results are compared with theoretical model calculations to gain insights into the underlying physics in the high baryon density region of the QCD phase diagram.

1 Introduction

Relativistic heavy-ion collisions offer a unique opportunity to investigate the properties and dynamical evolution of the deconfined phase of strongly interacting matter, commonly known as the Quark–Gluon Plasma (QGP) [1]. To study the transition from hadronic matter to the QGP and to map out the Quantum Chromodynamics (QCD) phase diagram, the Relativistic Heavy Ion Collider (RHIC) conducted the Beam Energy Scan (BES) program [2, 3].

One of the essential observables in this study is anisotropic flow, which captures the collective motion and shape of the expanding medium created in these collisions. Experimentally, this flow is observed as an anisotropy in the azimuthal distribution of particles with respect to the reaction plane and can be quantified through a Fourier expansion of the triple differential yield of final state particles:

$$E\frac{\mathrm{d}^3N}{\mathrm{d}p^3} = \frac{\mathrm{d}^2N}{2\pi p_T \mathrm{d}p_T \mathrm{d}y}\left\{1 + \sum_{n\geq 1} 2\,v_n\,\cos\left[n\left(\phi - \Psi_n\right)\right]\right\}, \tag{1}$$

where p_T is the transverse momentum, y is rapidity, ϕ is the particle's azimuthal angle, and Ψ_n is the n^{th}-order event plane angle [4]. The Fourier coefficients, v_n, describe how the medium collectively responds to the initial collision geometry. These coefficients are highly sensitive to the properties of the medium, including its viscosity and mean-field interactions, which govern the EoS [5].

In this proceedings, we will report the measurements of $v_1\{\Psi_1\}$, $v_2\{\Psi_2\}$, and $v_3\{\Psi_1\}$ for light, strange, multi-strange, net-particles, and light nuclei in Au+Au collisions. These measurements span energies of $\sqrt{s_{NN}}$ = 3.2 – 4.5 GeV conducted in fixed-target mode, as well as 7.7 – 19.6 GeV in collider mode, from the second phase of the Beam Energy Scan (BES-II) program at RHIC.

2 Analysis Details

The identification of charged particles in STAR is carried out using a combination of the Time Projection Chamber (TPC) and Time of Flight (TOF) detectors. The TPC provides information on the ionization energy loss (dE/dx), while the TOF uses timing information for particle

*e-mail: sharang.rav@students.iisertirupati.ac.in

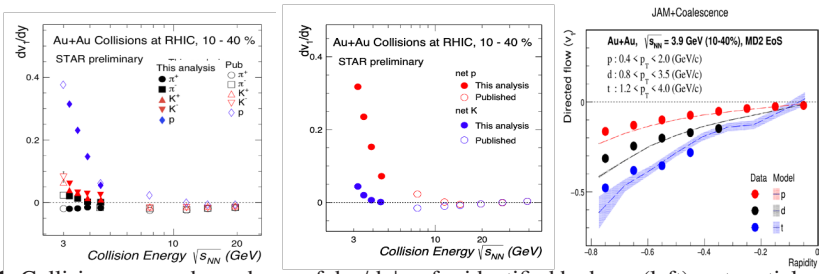

Figure 1. Collision energy dependence of $dv_1/dy|_{y=0}$ for identified hadrons (left), net particles (middle) in Au+Au collisions at RHIC for 10-40% centrality. The published data are shown in open markers [8, 9]. (Right) Rapidity dependence of v_1 for light nuclei in Au+Au collisions at $\sqrt{s_{NN}}$ = 3.2 GeV, with bands representing the JAM (momentum-dependent) mean-field calculation (κ = 380 MeV) with a coalescence afterburner.

identification [7]. The anisotropic flow coefficients are obtained from the azimuthal angle of a particle relative to the event plane (EP). In experiments, the event plane is determined by measuring the azimuthal distribution of produced particles and calculating the flow vector ($\vec{Q}_n$) for a given harmonic n [4]. The event plane angle is defined as $\Psi_n = \frac{1}{n}\tan^{-1}\left(\frac{Q_{n,y}}{Q_{n,x}}\right)$. The flow coefficients v_n are then calculated as $v_n = \frac{\langle\cos[n(\phi-\Psi_n)]\rangle}{R_n}$, with R_n being the resolution of the n^{th}-order EP, determined using a three-sub-event plane correlation method [4].

3 Results and Discussions

3.1 Directed flow (v_1)

A minimum in the slope of the v_1 of baryons at mid-rapidity, $dv_1/dy|_{y=0}$, as a function of collision energy has been proposed as a possible signature of a first-order phase transition between the QGP and the hadronic phase [5, 6]. In this study, we present detailed measurements of v_1 for identified hadrons, net-particles, and light nuclei in Au+Au collisions at $\sqrt{s_{NN}}$ = 3.2–4.5 GeV. The left and middle panels of Fig. 1 show the collision energy dependence of v_1 slope for identified hadrons and net-particles. It is observed that the slope of v_1 decreases with increasing collision energy for all studied particles. Additionally, a splitting between π^+ and π^- appears, which is attributed to spectator shadowing effects at lower energies. The net-kaon $dv_1/dy|_{y=0}$ shows a minimum in the range $\sqrt{s_{NN}}$ = 4.5 – 7.7 GeV, which is lower than the minimum for net-protons, found between $\sqrt{s_{NN}}$ = 11.5 – 19.6 GeV [8]. The right panel of Fig. 1 shows the rapidity dependence of v_1 for light nuclei in Au+Au collisions at $\sqrt{s_{NN}}$ = 3.2 GeV, along with JAM model calculations with a mean-field and a coalescence afterburner. It is observed that the model provides a good description of the experimental trends, highlighting the importance of mean-field effects and coalescence as the dominant production mechanism for light nuclei at low energies. The ϕ meson, an especially interesting probe because it is a meson with baryon-like mass, is also studied. Figure 2 shows the v_1 slope for ϕ along with other mesons and baryons. It is observed that the v_1 slope of the ϕ meson exhibits a baryon-like pattern rather than a typical meson-like behaviour at low collision energies

To investigate anti-flow of mesons at low collision energies, arising from the relatively long spectator passage time, a p_T dependence of the v_1 slope is studied and is plotted in the left panel of Fig. 2, and anti-flow is observed at low p_T. Comparisons with JAM model calculations in the cascade mode, both with and without spectators, reveal that spectator nucleons play a decisive role in producing the observed meson anti-flow. This indicates that the effect can be explained without invoking an additional kaon potential, contrary to earlier assumptions [11].

3.2 Elliptic flow (v_2)

Partonic collectivity is considered a key signature for the formation of the QGP in high-energy heavy-ion collisions [13]. The scaling of v_2 with the Number of Constituent Quarks (NCQ)

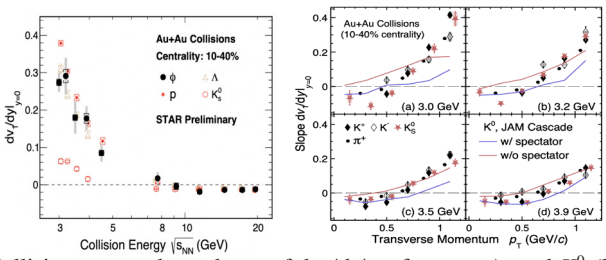

Figure 2. (Left) Collision energy dependence of $dv_1/dy|_{y=0}$ for p, ϕ, Λ, and K^0_S (left panel) in Au+Au collisions at RHIC for 10-40% centrality. (Right) The p_T dependence of $dv_1/dy|_{y=0}$ for mesons in Au+Au collisions at $\sqrt{s_{NN}}$ = 3.0 - 3.9 GeV. Markers indicate the experimental data, whereas the lines represent the JAM model calculations [10].

has been observed for light and strange hadrons at top RHIC energies and is widely regarded as strong evidence of collectivity at the partonic level. However, this scaling behavior disappears at lower energies, such as $\sqrt{s_{NN}}$ = 3 GeV [9, 13]. In this work, the v_2 of various particles and their antiparticles is studied in Au+Au collisions spanning $\sqrt{s_{NN}}$ = 3.0 - 19.6 GeV to investigate the onset of NCQ scaling. Figure 3 shows the NCQ scaled v_2 for anti-particles in Au+Au collisions at $\sqrt{s_{NN}}$ = 3.0–19.6 GeV. It is observed that below about 3.2 GeV, the NCQ scaling breaks down completely, while at higher energies it progressively restores. This breakdown indicates a shift in the dominant degrees of freedom from hadronic to partonic matter, marking an important threshold for the onset of partonic collectivity at lower collision energies. It has also been observed that at 3.0 GeV, hadronic transport models (JAM, AMPT-HC, SMASH) qualitatively describe the v_2 data, while at 4.5 GeV they underestimate it, with AMPT-SM (including partonic interactions) providing a better description [14].

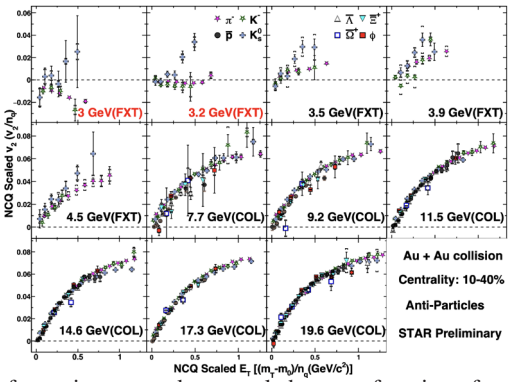

Figure 3. The number of constituent quarks n_q scaled v_2 as a function of n_q scaled transverse kinetic energy for anti-particles in Au+Au collisions at $\sqrt{s_{NN}}$ = 3.0 - 19.6 GeV.

3.3 Triangular flow (v_3)

At high collision energies, v_3 mainly arises from event-by-event geometric fluctuations that are uncorrelated with the reaction plane. Since these triangular fluctuations can point in any direction relative to Ψ_r, the conventional v_3 is measured with respect to the third-order event plane Ψ_3. However, at lower collision energies, experimental observations by the HADES experiment at 2.4 GeV and STAR at 3 GeV have revealed a surprising correlation between v_3 and the first-order event plane (Ψ_1) [16, 17]. This correlation is believed to result from the combined influence of the initial collision geometry and the mean-field potential within the medium. To investigate this further, a systematic study of $v_3\{\Psi_1\}$ has been performed for Au+Au collisions at $\sqrt{s_{NN}}$ = 3.2–4.5 GeV. The rapidity dependence of v_3, along with JAM

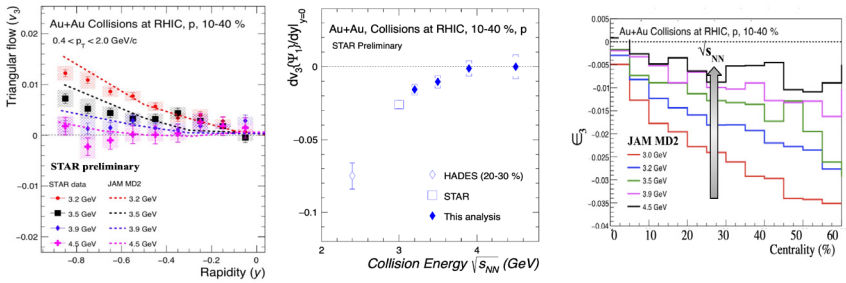

Figure 4. (Left) Rapidity dependence of $v_3\{\Psi_1\}$ in Au+Au collisions at $\sqrt{s_{NN}}$ = 3.2–4.5 GeV. (Middle) Collision energy dependence of the $v_3\{\Psi_1\}$ slope in Au+Au collisions. (Right) Centrality dependence of the initial triangularity ϵ_3 in mid-rapidity region (-0.5 < y < 0) of Au+Au collisions at t = 20 fm/c.

model predictions incorporating a mean-field potential, is shown in the left panel of Fig. 4. The comparison highlights that the inclusion of a mean-field potential is essential for reproducing the experimental observations. Complementary studies (not presented here) further indicate that its absence results in a substantial underestimation of the measured signal [18]. To quantify the strength of the signal, the slope of $v_3\{\Psi_1\}$, $dv_3\{\Psi_1\}/dy|_{y=0}$ has been extracted and is presented in the middle panel of Fig. 4. The results show that the slope gradually decreases with increasing collision energy and approaches zero near 4.5 GeV. Additionally, by analogy with eccentricity for elliptic flow, the triangularity (ϵ_3) is calculated and is plotted as a function of centrality in the right panel of Fig. 4. The ϵ_3 increases towards more peripheral collisions and decreases with higher energies. This qualitative trend is clearly reflected in the experimental data, highlighting the key role of the initial collision geometry, as quantified by ϵ_3, in the development of the observed $v_3\{\Psi_1\}$ signal.

References

[1] J. Adams et al. (STAR Collaboration), Nucl. Phys. A **757**, 102 (2005).
[2] B. Mohanty, Nucl. Phys. A **830**, 899c (2009).
[3] J. Chen, et al., Nucl. Sci. Tech. **35**, 12 (2024)
[4] A. M. Poskanzer and S. A. Voloshin, Phys. Rev. C **58**, 1671 (1998).
[5] H. Stocker, Nucl. Phys. A **750**, 121 (2005).
[6] L. Adamczyk et al. (STAR Collaboration), Phys. Rev. Lett. **112**, 162301 (2014).
[7] L. Adamczyk et al. (STAR Collaboration), Phys. Rev. C **96**, 044904 (2017).
[8] L. Adamczyk et al. (STAR Collaboration), Phys. Rev. Lett. **120**, 062301 (2018).
[9] M. S. Abdallah et al. (STAR Collaboration), Phys. Lett. B 827, 137003 (2022).
[10] STAR Collaboration, arXiv:2503.23665 [nucl-ex].
[11] P. Chung et al. (E895 Collaboration), Phys. Rev. Lett. **85**, 940 (2000).
[12] Y. Nara, H. Niemi, A. Ohnishi, and H. Stocker, Phys. Rev. C **94**, 034906 (2016).
[13] P. Braun-Munzinger and J. Stachel, Nature 448, 301 (2007)
[14] STAR Collaboration, arXiv:2504.02531 [nucl-ex] (2025).
[15] L. Adamczyk et al. (STAR), Phys. Rev. C 93, 014907 (2016).
[16] J. Adamczewski-Musch et al. (HADES Collaboration), Phys. Rev. Lett. **125**, 262301 (2020).
[17] M. I. Abdulhamid et al. (STAR Collaboration), Phys. Rev. C **109**, 044914 (2024).
[18] S.R. Sharma (STAR Collaboration), J.Subatomic Part. Cosmol. 4 (2025) 100102.